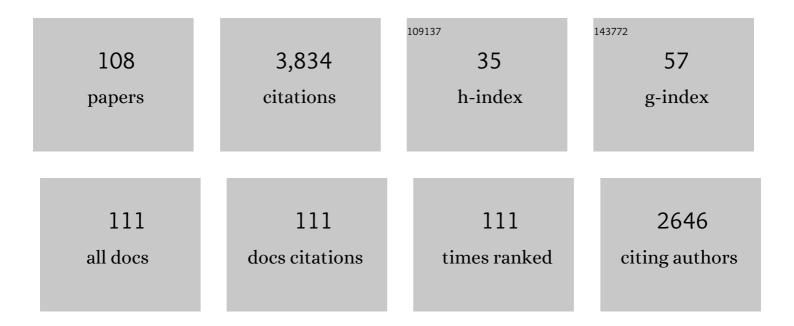
## Michel Cathelineau

List of Publications by Year in descending order

Source: https://exaly.com/author-pdf/11901154/publications.pdf Version: 2024-02-01



#	Article	IF	CITATIONS
1	A chlorite solid solution geothermometer the Los Azufres (Mexico) geothermal system. Contributions To Mineralogy and Petrology, 1985, 91, 235-244.	1.2	560
2	The Hydrothermal Alkali Metasomatism Effects on Granitic Rocks: Quartz Dissolution and Related Subsolidus Changes. Journal of Petrology, 1986, 27, 945-965.	1.1	126
3	Giant uranium deposits formed from exceptionally uranium-rich acidic brines. Nature Geoscience, 2012, 5, 142-146.	5.4	107
4	Low-temperature chlorite geothermometry: a graphical representation based on a T–R2+ –Si diagram. European Journal of Mineralogy, 2015, 27, 617-626.	0.4	105
5	An evaporated seawater origin for the ore-forming brines in unconformity-related uranium deposits (Athabasca Basin, Canada): Cl/Br and δ37Cl analysis of fluid inclusions. Geochimica Et Cosmochimica Acta, 2011, 75, 2792-2810.	1.6	104
6	Mixing of metamorphic and surficial fluids during the uplift of the Hercynian upper crust: consequences for gold deposition. Chemical Geology, 2003, 194, 119-141.	1.4	95
7	Improvements in clathrate modelling: I. The H2O-CO2 system with various salts. Geochimica Et Cosmochimica Acta, 1996, 60, 1657-1681.	1.6	90
8	Paleo-fluid composition determined from individual fluid inclusions by Raman and LIBS: Application to mid-proterozoic evaporitic Na–Ca brines (Alligator Rivers Uranium Field, northern territories) Tj ETQq0 0 0 rgB1	ſ <b>∕0</b> ,∡erlock	: 1 <b>10</b> 1 Tf 50 45
9	Migration of brines in the basement rocks of the Athabasca Basin through microfracture networks (P-Patch U deposit, Canada). Lithos, 2010, 115, 121-136.	0.6	66
10	A reinvestigation of smectite illitization in experimental hydrothermal conditions: Results from X-ray diffraction and transmission electron microscopy. American Mineralogist, 2011, 96, 207-223.	0.9	66
11	Effects of Temperature, pH, and Iron/Clay and Liquid/Clay Ratios on Experimental Conversion of Dioctahedral Smectite to Berthierine, Chlorite, Vermiculite, or Saponite. Clays and Clay Minerals, 2010, 58, 280-291.	0.6	65
12	A detailed fluid inclusion study in silicified breccias from the Kombolgie sandstones (Northern) Tj ETQq0 0 0 rgBT deposits. Journal of Geochemical Exploration, 2003, 80, 259-275.	/Overlock 1.5	10 Tf 50 30 64
13	Metallogenesis of the French part of the Variscan orogen. Part II: Time-space relationships between U, Au and Snî—,W ore deposition and geodynamic events — mineralogical and Uî—,Pb data. Tectonophysics, 1990, 177, 59-79.	0.9	63
14	Evidence for Li-rich brines and early magmatic fluid-rock interactionin the Larderello geothermal system. Geochimica Et Cosmochimica Acta, 1994, 58, 1083-1099.	1.6	62
15	Metal-rich fluid inclusions provide new insights into unconformity-related U deposits (Athabasca) Tj ETQq1 1 0.7	84314 rgB 1.7	T /Overlock
16	A major Late Jurassic fluid event at the basin/basement unconformity in western France: 40Ar/39Ar and K–Ar dating, fluid chemistry, and related geodynamic context. Chemical Geology, 2012, 322-323, 99-120.	1.4	60
17	Clay minerals trap hydrogen in the Earth's crust: Evidence from the Cigar Lake uranium deposit, Athabasca. Earth and Planetary Science Letters, 2018, 493, 186-197.	1.8	60
18	Boron- and magnesium-rich marine brines at the origin of giant unconformity-related uranium deposits: δ11B evidence from Mg-tourmalines. Geology, 2012, 40, 231-234.	2.0	57

#	Article	IF	CITATIONS
19	Penetration of surface-evaporated brines into the Proterozoic basement and deposition of Co and Ag at Bou Azzer (Morocco): Evidence from fluid inclusions. Journal of African Earth Sciences, 2005, 41, 25-39.	0.9	55
20	The relative distribution of critical (Sc, REE) and transition metals (Ni, Co, Cr, Mn, V) in some Ni-laterite deposits of New Caledonia. Journal of Geochemical Exploration, 2019, 197, 93-113.	1.5	50
21	Conditions of gold-bearing arsenopyrite crystallization in the Villeranges Basin, Marche-Combrailles shear zone, France; a mineralogical and fluid inclusion study. Economic Geology, 1989, 84, 1340-1362.	1.8	46
22	Microfracturing and fluid mixing in granites: W–(Sn) ore deposition at Vaulry (NW French Massif) Tj ETQq0 0	0 rgBT /O	verlock 10 Tf 5
23	Reconstruction of low temperature (<100°C) burial in sedimentary basins: A comparison of geothermometer in the intracontinental Paris Basin. Marine and Petroleum Geology, 2014, 53, 71-87.	1.5	46
24	Pressure fluctuation during uplift of the Northern Apennines (Italy): a fluid inclusions study. Tectonophysics, 2001, 341, 121-139.	0.9	45
25	Remobilisation of base metals and gold by Variscan metamorphic fluids in the south Iberian pyrite belt: evidence from the Tharsis VMS deposit. Chemical Geology, 2003, 194, 143-165.	1.4	45
26	Temperature of paleo- to modern self-sealing within a continental rift basin: The fluid inclusion data (Soultz-sous-Forêts, Rhine graben, France). European Journal of Mineralogy, 1996, 8, 1065-1080.	0.4	45
27	U redox fronts and kaolinisation in basement-hosted unconformity-related U ores of the Athabasca Basin (Canada): late U remobilisation by meteoric fluids. Mineralium Deposita, 2011, 46, 105-135.	1.7	44
28	From evaporated seawater to uranium-mineralizing brines: Isotopic and trace element study of quartz–dolomite veins in the Athabasca system. Geochimica Et Cosmochimica Acta, 2013, 113, 38-59.	1.6	44
29	Syn-tectonic, meteoric water–derived carbonation of the New Caledonia peridotite nappe. Geology, 2013, 41, 1063-1066.	2.0	41
30	Boiling and fluid mixing in the chlorite zone of the Larderello geothermal system. Chemical Geology, 1999, 154, 237-256.	1.4	38
31	Geometry and P–V–T–X conditions of microfissural ore fluid migration: the Mokrsko gold deposit (Bohemia). Chemical Geology, 2001, 173, 207-225.	1.4	38
32	Dissolution–precipitation processes governing the carbonation and silicification of the serpentinite sole of the New Caledonia ophiolite. Contributions To Mineralogy and Petrology, 2014, 167, 1.	1.2	38
33	Formation of U-rich mineralizing fluids through basinal brine migration within basement-hosted shear zones: A large-scale study of the fluid chemistry around the unconformity-related Cigar Lake U deposit (Saskatchewan, Canada). Chemical Geology, 2019, 508, 116-143.	1.4	37
34	Dating multistage paleofluid percolations: A K-Ar and 18O/16O study of fracture illites from altered Hercynian plutonites at the basement/cover interface (Poitou High, France). Geochimica Et Cosmochimica Acta, 2004, 68, 2529-2542.	1.6	36
35	Basinal Brines at the Origin of the Imiter Ag-Hg Deposit (Anti-Atlas, Morocco): Evidence from LA-ICP-MS Data on Fluid Inclusions, Halogen Signatures, and Stable Isotopes (H, C, O). Economic Geology, 2016, 111, 1753-1781.	1.8	36
36	Nickel dispersion and enrichment at the bottom of the regolith: formation of pimelite target-like ores in rock block joints (Koniambo Ni deposit, New Caledonia). Mineralium Deposita, 2016, 51, 271-282.	1.7	36

#	Article	IF	CITATIONS
37	Fluid inclusion evidence of the differential migration of H2 and O2in the McArthur River unconformity-type uranium deposit (Saskatchewan, Canada). Possible role on post-ore modifications of the host rocks. Journal of Geochemical Exploration, 2003, 78-79, 525-530.	1.5	35
38	Detailed determination of palaeofluid chemistry: an integrated study of sulphate-volatile rich brines and aquo-carbonic fluids in quartz veins from Ouro Fino (Brazil). Chemical Geology, 1999, 154, 179-192.	1.4	34
39	Noble gases (Ar, Kr, Xe) and halogens (Cl, Br, I) in fluid inclusions from the Athabasca Basin (Canada): Implications for unconformity-related U deposits. Precambrian Research, 2014, 247, 110-125.	1.2	34
40	Chronology of fracture sealing under a meteoric fluid environment: Microtectonic and isotopic evidence of major Cainozoic events in the eastern Paris Basin (France). Tectonophysics, 2010, 490, 214-228.	0.9	33
41	Paired stable isotopes (O, C) and clumped isotope thermometry of magnesite and silica veins in the New Caledonia Peridotite Nappe. Geochimica Et Cosmochimica Acta, 2016, 183, 234-249.	1.6	33
42	Brine-rock interaction in the Athabasca basement (McArthur River U deposit, Canada): consequences for fluid chemistry and uranium uptake. Terra Nova, 2010, 22, no-no.	0.9	32
43	Revealing the conditions of Ni mineralization in the laterite profiles of New Caledonia: Insights from reactive geochemical transport modelling. Chemical Geology, 2017, 466, 274-284.	1.4	32
44	The granite hosted gold deposit of Moulin de Ch�ni (Saint-Yrieix district, Massif Central, France): petrographic, structural, fluid inclusion and oxygen isotope constraints. Mineralium Deposita, 2004, 39, 265-281.	1.7	31
45	Impact of basin burial and exhumation on Jurassic carbonates diagenesis on both sides of a thick clay barrier (Paris Basin, NE France). Marine and Petroleum Geology, 2014, 53, 44-70.	1.5	31
46	Post-crystallization alteration of natural uraninites: Implications for dating, tracing, and nuclear forensics. Geochimica Et Cosmochimica Acta, 2019, 249, 138-159.	1.6	31
47	Multistage crack seal vein and hydrothermal Ni enrichment in serpentinized ultramafic rocks (Koniambo massif, New Caledonia). Mineralium Deposita, 2017, 52, 945-960.	1.7	28
48	The internal deformation of the Peridotite Nappe of New Caledonia: A structural study of serpentine-bearing faults and shear zones in the Koniambo Massif. Journal of Structural Geology, 2016, 85, 51-67.	1.0	27
49	The Role of Organic Matter on Uranium Precipitation in Zoovch Ovoo, Mongolia. Minerals (Basel,) Tj ETQq1 1 0.3	784314 rg 0.8	gBT /Overlock 27
50	Fluid inclusions in granites and their relationships with present-day groundwater chemistry. European Journal of Mineralogy, 1998, 10, 1215-1226.	0.4	27
51	Uranium mineralization in the Alum Shale Formation (Sweden): Evolution of a U-rich marine black shale from sedimentation to metamorphism. Ore Geology Reviews, 2017, 88, 71-98.	1.1	26
52	Fluid pressure variations in relation to multistage deformation and uplift: a fluid inclusion study of Au quartz veins. European Journal of Mineralogy, 1993, 5, 107-122.	0.4	26
53	Raman spectra of Ni–Mg kerolite: effect of Ni–Mg substitution on O–H stretching vibrations. Journal of Raman Spectroscopy, 2015, 46, 933-940.	1.2	24
54	3D modeling of the laterites on top of the Koniambo Massif, New Caledonia: refinement of the per descensum lateritic model for nickel mineralization. Mineralium Deposita, 2017, 52, 961-978.	1.7	24

MICHEL CATHELINEAU

#	Article	IF	CITATIONS
55	Rutile from Panasqueira (Central Portugal): An Excellent Pathfinder for Wolframite Deposition. Minerals (Basel, Switzerland), 2019, 9, 9.	0.8	24
56	Characterization of Weda Bay nickel laterite ore from Indonesia. Journal of Geochemical Exploration, 2019, 196, 270-281.	1.5	24
57	Experimental illitization of smectite in a K-rich solution. European Journal of Mineralogy, 2001, 13, 829-840.	0.4	23
58	Downward penetration and mixing of sedimentary brines and dilute hot waters at 5â€km depth in the granite basement at Soultz-sous-Forêts (Rhine graben, France). Comptes Rendus - Geoscience, 2010, 342, 560-565.	0.4	23
59	Poultry litter ash characterisation and recovery. Waste Management, 2020, 111, 10-21.	3.7	22
60	Reconstructing fluid-flow events in Lower-Triassic sandstones of the eastern Paris Basin by elemental tracing and isotopic dating of nanometric illite crystals. Geochimica Et Cosmochimica Acta, 2016, 176, 157-184.	1.6	21
61	Alpine metamorphism and veining in the Zentralgneis Complex of the SW Tauern Window: a model of fluid–rock interactions based on fluid inclusions. Tectonophysics, 2001, 336, 121-136.	0.9	20
62	Active contact metamorphism and CO2–CH4 fluid production in the Larderello geothermal field (Italy) at depths between 2.3 and 4Âkm. Chemical Geology, 2007, 237, 303-328.	1.4	20
63	The emplacement of the Peridotite Nappe of New Caledonia and its bearing on the tectonics of obduction. Tectonics, 2016, 35, 3070-3094.	1.3	19
64	Mineralogical Evolution of a Claystone After Reaction With Iron Under Thermal Gradient. Clays and Clay Minerals, 2012, 60, 443-455.	0.6	18
65	Uraniferous bitumen nodules in the Talvivaara Ni–Zn–Cu–Co deposit (Finland): influence of metamorphism on uranium mineralization in black shales. Mineralium Deposita, 2014, 49, 513-533.	1.7	18
66	Hot Fluid Flows Around A Major Fault Identified By Paleothermometric Studies (Tim MersoÃ <sup>-</sup> Basin,) Tj ETQq0 0	0 rgBT /Ov	erlogk 10 Tf 5
67	C-O-H-N fluids circulations and graphite precipitation in reactivated Hudsonian shear zones during basement uplift of the Wollaston-Mudjatik Transition Zone: Example of the Cigar Lake U deposit. Lithos, 2017, 294-295, 222-245.	0.6	18
68	Mineralogy and ore fluid chemistry of the Roc Blanc Ag deposit, Jebilet Hercynian massif, Morocco. Journal of African Earth Sciences, 2017, 127, 175-193.	0.9	18
69	Multistage evolution of the Pierres-Plantées uranium ore deposit (Margeride, France): evidence from mineralogy and U-Pb systematics. European Journal of Mineralogy, 1991, 3, 85-104.	0.4	18
70	Serpentinization of New Caledonia peridotites: from depth to (sub-)surface. Contributions To Mineralogy and Petrology, 2020, 175, 1.	1.2	17
71	In-situ Isotopic and Chemical Study of Pyrite from Chu-Sarysu (Kazakhstan) Roll-front Uranium Deposit. Procedia Earth and Planetary Science, 2015, 13, 207-210.	0.6	16
72	Weathering processes and crystal chemistry of Ni-bearing minerals in saprock horizons of New Caledonia ophiolite. Journal of Geochemical Exploration, 2019, 198, 82-99.	1.5	16

#	Article	IF	CITATIONS
73	The Panasqueira Rare Metal Granite Suites and Their Involvement in the Genesis of the World-Class Panasqueira W–Sn–Cu Vein Deposit: A Petrographic, Mineralogical, and Geochemical Study. Minerals (Basel, Switzerland), 2020, 10, 562.	0.8	16
74	Brines related to Ag deposition in the Zgounder silver deposit (Anti-Atlas, Morocco). European Journal of Mineralogy, 1998, 10, 1201-1214.	0.4	16
75	Contribution of long-term hydrothermal experiments for understanding the smectite-to-chlorite conversion in geological environments. Contributions To Mineralogy and Petrology, 2016, 171, 1.	1.2	15
76	Nature and Origin of Mineralizing Fluids in Hyperextensional Systems: The Case of Cretaceous Mg Metasomatism in the Pyrenees. Geofluids, 2019, 2019, 1-18.	0.3	14
77	Effect of a Thermal Gradient on Iron-Clay Interactions. Clays and Clay Minerals, 2010, 58, 667-681.	0.6	13
78	Uranium deposits of Franceville basin (Gabon): Role of organic matter and oil cracking on uranium mineralization. Ore Geology Reviews, 2020, 123, 103579.	1.1	13
79	Monazite Alteration in H2O ± HCl ± NaCl ± CaCl2 Fluids at 150 ºC and psat: Implications for Uranium Deposits. Minerals (Basel, Switzerland), 2015, 5, 693-706.	0.8	13
80	Vertical and lateral changes in organic matter from the Mesozoic, eastern Paris Basin (France): Variability of sources and burial history. International Journal of Coal Geology, 2011, 88, 163-178.	1.9	12
81	A multi-analytical approach to the study of uranium-ore agglomerate structure and porosity during heap leaching. Hydrometallurgy, 2017, 171, 33-43.	1.8	12
82	High pressure and temperatures during the early stages of tungsten deposition at Panasqueira revealed by fluid inclusions in topaz. Ore Geology Reviews, 2020, 126, 103741.	1.1	12
83	llmenites and their alteration products, sinkholes for uranium and radium in roll-front deposits after the example of South Tortkuduk (Kazakhstan). Journal of Geochemical Exploration, 2019, 206, 106343.	1.5	11
84	Oxfordian sedimentary dykes : tectonic and diagenetic implications for the eastern Paris basin. Bulletin - Societie Geologique De France, 2004, 175, 595-605.	0.9	9
85	Tungsten (VI) speciation in hydrothermal solutions up to 400°C as revealed by in-situ Raman spectroscopy. Geochimica Et Cosmochimica Acta, 2022, 317, 306-324.	1.6	9
86	Evolution of porewater composition through time in limestone aquifers: Salinity and D/H of fluid inclusion water in authigenic minerals (Jurassic of the eastern Paris Basin, France). Chemical Geology, 2015, 417, 210-227.	1.4	8
87	Reappraisal of the GLâ€O Reference Material for Kâ€Ar Dating: New Insight from Microanalysis, Singleâ€Grain and Milligram Ar Measurements. Geostandards and Geoanalytical Research, 2020, 44, 287-306.	1.7	8
88	Evaporitic brines and copper-sulphide ore genesis at Jbel HaÃ⁻mer (Central Jebilet, Morocco). Ore Geology Reviews, 2021, 129, 103920.	1.1	7
89	Incineration of Aviary Manure: The Case Studies of Poultry Litter and Laying Hens Manure. Waste and Biomass Valorization, 2022, 13, 3335-3357.	1.8	7
90	Conditioning of poultry manure ash for subsequent phosphorous separation and assessment for a process design. Sustainable Materials and Technologies, 2022, 31, e00377.	1.7	6

MICHEL CATHELINEAU

#	Article	IF	CITATIONS
91	Reactive Transport Modeling Applied to Ni Laterite Ore Deposits in New Caledonia: Role of Hydrodynamic Factors and Geological Structures in Ni Mineralization. Geochemistry, Geophysics, Geosystems, 2019, 20, 1425-1440.	1.0	5
92	Tracing metallic pre-concentrations in the Limousin ophiolite-derived rocks and Variscan granites (French Massif Central). Lithos, 2020, 356-357, 105345.	0.6	5
93	Conditions for uranium biomineralization during the formation of the Zoovch Ovoo roll-front-type uranium deposit in East Gobi Basin, Mongolia. Ore Geology Reviews, 2021, 138, 104351.	1.1	5
94	Multiscale physical–chemical analysis of the impact of fracture networks on weathering: Application to nickel redistribution in the formation of Ni-laterite ores, New Caledonia. Ore Geology Reviews, 2022, 147, 104971.	1.1	5
95	Comment on the paper by Sanchez-España et al.: source and evolution of ore-forming hydrothermal fluids in the northern Iberian pyrite belt massive sulphide deposits (SW Spain): evidence from fluid inclusions and stable isotopes (Mineralium Deposita 38: 519–537). Mineralium Deposita, 2006, 40, 742-748.	1.7	4
96	Basinal Brines at the Origin of the Imiter Ag-Hg Deposit (Anti-Atlas, Morocco): Evidence from LA-ICP-MS Data on Fluid Inclusions, Halogen Signatures, and Stable Isotopes (H, C, O)—A Reply. Economic Geology, 2017, 112, 1273-1277.	1.8	4
97	Metamorphic brines and no surficial fluids trapped in the detachment footwall of a Metamorphic Core Complex (Nevado-Filábride units, Betics, Spain). Tectonophysics, 2018, 727, 56-72.	0.9	4
98	A study of uranium-ore agglomeration parameters and their implications during heap leaching. Minerals Engineering, 2018, 127, 22-31.	1.8	4
99	An integrated multiscale approach to heap leaching of uranium-ore agglomerates. Hydrometallurgy, 2018, 178, 274-282.	1.8	4
100	Cenozoic oxidation episodes in West Africa at the origin of the in situ supergene mineral redistribution of the primary uranium orebodies (Imouraren deposit, Tim MersoÃ <sup>-</sup> Basin, Northern) Tj ETQq0 0 0 rg	g <b>BiT7</b> /Overl	oek 10 Tf 50
101	Near real-time management of spectral interferences with portable X-ray fluorescence spectrometers: application to Sc quantification in nickeliferous laterite ores. Geochemistry: Exploration, Environment, Analysis, 2021, 21, .	0.5	4
102	Evaluation of Sc Concentrations in Ni-Co Laterites Using Al as a Geochemical Proxy. Minerals (Basel,) Tj ETQq0 0 (	ΩrgBT /Ον	erlock 10 Tf
103	Dolomite cements in Cenomanian continental sand deposits: Time evolution and significance (Zoovch) Tj ETQq1	1 0.78431 1.0	.4 rgBT /Ove
104	Evaporitic brines and copper-sulphide ore genesis at Jbel HaÃ <sup>-</sup> mer (Central Jebilet, Morocco): A reply. Ore Geology Reviews, 2021, 140, 104409.	1.1	1
105	Origin of 87Sr enrichment in calcite cements in Jurassic limestones (Eastern Paris Basin, France). Applied Geochemistry, 2021, 136, 105131.	1.4	1
106	Significance of H2 and CO release during thermal treatment of natural phyllosilicate-rich rocks. Chemical Geology, 2022, 588, 120647.	1.4	1
107	Comment on the paper by Sanchez-Espa�a et al.: Source and evolution of ore-forming hydrothermal fluids in the northern Iberian Pyrite Belt massive sulphide deposits (SW Spain): evidence from fluid inclusions and stable isotopes (Mineralium Deposita 38:519?537). Mineralium Deposita, 2006, 40, 742.	1.7	0
108	The Tim MersoÃ <sup>–</sup> Basin uranium deposits (Northern Niger): Geochronology and genetic model. Ore Geology Reviews, 2022, 145, 104905.	1.1	0